JCB Article

A novel mechanism of myocyte degeneration involving the Ca^{2+}-permeable growth factor–regulated channel

Yuko Iwata,[1] Yuki Katanosaka,[1] Yuji Arai,[2] Kazuo Komamura,[3] Kunio Miyatake,[4] and Munekazu Shigekawa[1]

[1]Department of Molecular Physiology, [2]Department of Bioscience, and [3]Department of Cardiovascular Dynamics, National Cardiovascular Center Research Institute, and [4]Division of Cardiology, National Cardiovascular Center Hospital, Suita, Osaka 565-8565, Japan

Disruption of the dystrophin–glycoprotein complex caused by genetic defects of dystrophin or sarcoglycans results in muscular dystrophy and/or cardiomyopathy in humans and animal models. However, the key early molecular events leading to myocyte degeneration remain elusive. Here, we observed that the growth factor–regulated channel (GRC), which belongs to the transient receptor potential channel family, is elevated in the sarcolemma of skeletal and/or cardiac muscle in dystrophic human patients and animal models deficient in dystrophin or δ-sarcoglycan. However, total cell GRC does not differ markedly between normal and dystrophic muscles. Analysis of the properties of myotubes prepared from δ-sarcoglycan–deficient BIO14.6 hamsters revealed that GRC is activated in response to myocyte stretch and is responsible for enhanced Ca^{2+} influx and resultant cell damage as measured by creatine phosphokinase efflux. We found that cell stretch increases GRC translocation to the sarcolemma, which requires entry of external Ca^{2+}. Consistent with these findings, cardiac-specific expression of GRC in a transgenic mouse model produced cardiomyopathy due to Ca^{2+} overloading, with disease expression roughly parallel to sarcolemmal GRC levels. The results suggest that GRC is a key player in the pathogenesis of myocyte degeneration caused by dystrophin–glycoprotein complex disruption.

Introduction

In striated muscle fibers, dystrophin forms a trans-sarcolemmal complex with its associated proteins, i.e., the intrinsic membrane glycoproteins β-dystroglycan and α-, β-, γ-, and δ-sarcoglycans (δ-SGs),* as well as several nonmembrane proteins (Straub and Campbell, 1997; Ozawa et al., 1998). This large oligomeric composite, named the dystrophin–glycoprotein complex (DGC), links the intracellular actin cytoskeleton to the overlying basal lamina, thereby providing structural support for the sarcolemma. The functional importance of the DGC is underscored by the fact that genetic defects in its major components (dystrophin and sarcoglycans) disrupt the complex, leading to muscular dystrophy and/or cardiomyopathy in humans and animal models (Straub and Campbell, 1997; Ozawa et al., 1998; Towbin and Bawles, 2002).

The mechanism by which a defective DGC causes myocyte degeneration still remains elusive. Myocyte degeneration has long been attributed to membrane defects such as greater fragility toward mechanical stress (Mokri and Engel, 1975; Menke and Jockusch, 1991; Petrof et al., 1993) or increased permeability to Ca^{2+} (Fong et al., 1990; Tutdibi et al., 1999; Alderton and Steinhardt, 2000b). A number of studies have reported chronic elevation of $[Ca^{2+}]$ in the cytosol ($[Ca^{2+}]_i$), beneath the sarcolemma, or within other cell compartments in skeletal muscle fibers and cultured myotubes from dystrophin-deficient Duchenne muscular dystrophy (DMD) patients and *mdx* mice (a mouse model of DMD; Brown and Lucy, 1997; Mallouk et al., 2000; Robert et al., 2001), although elevation of resting $[Ca^{2+}]_i$ has often been disputed. Enhanced Ca^{2+} entry into dystrophic myocytes is consistent with previous demonstrations of sustained activation of sarcolemmal Ca^{2+}-permeable channels (a Ca^{2+}-specific leak channel [Fong et al., 1990; Alderton and Steinhardt, 2000b] or a mechanosensitive nonselective cation channel [Franco-Obregon and Lansman, 1994; Vandebrouck et al., 2001]).

The BIO14.6 strain of the Syrian hamster develops severe cardiomyopathy and muscular dystrophy due to a genetic

Y. Iwata and Y. Katanosaka contributed equally to this work.

Address correspondence to Munekazu Shigekawa, Dept. of Molecular Physiology, National Cardiovascular Center Research Institute, Fujishiro-dai 5-7-1, Suita, Osaka 565-8565, Japan. Tel.: 81-6-6833-5012. Fax: 81-6-6835-5314. E-mail: shigekaw@ri.ncvc.go.jp

*Abbreviations used in this paper: β-gal, β-galactosidase; CK, creatine phosphokinase; DGC, dystrophin–glycoprotein complex; DMD, Duchenne muscular dystrophy; δ-SG, δ-sarcoglycan; GRC, growth factor–regulated channel; NHS-biotin, *N*-hydroxysuccinimido-biotin; TRP, transient receptor potential.

Key words: dystrophin–glycoprotein complex; muscular dystrophy; cardiomyopathy; nonselective cation channel; calcium entry

defect in its δ-SG, and usually dies of congestive heart failure (Bajusz et al., 1969; Nigro et al., 1997). In this model, the DGC is disrupted because δ-SG deficiency causes secondary reduction of other sarcoglycans and α-dystroglycan in the sarcolemma, whereas dystrophin and β-dystroglycan are still retained at one half of their normal levels (Iwata et al., 1993). We have shown in recent work that stretch-sensitive cation-selective channels similar to those recorded in *mdx* skeletal muscle are active in resting cultured myotubes prepared from BIO14.6 hamster (Nakamura et al., 2001).

To identify Ca^{2+} entry mechanisms possibly responsible for the pathogenesis of myocyte degeneration, we undertook a search for mammalian homologues of the *Drosophila* transient receptor potential (TRP) channel expressed in striated muscle, because this family of channels contains a subfamily of Ca^{2+}-permeable cation channels sensitive to physical stimuli, such as osmotic stress or heat (Montell and Birnbaumer, 2002). Here, we report that the growth factor–regulated channel (GRC) belonging to the TRP family (Kanzaki et al., 1999) and being possibly a mouse homologue of VRL1 (Caterina et al., 1999), is abundantly expressed in the sarcolemma of cardiac or skeletal myocytes with defective dystrophin or δ-SG. GRC, which was originally identified as a Ca^{2+}-permeable nonselective cation channel expressed in nonmuscle cells, localizes mainly in intracellular pools under basal conditions and translocates to the cell surface on stimulation with growth factors (Kanzaki et al., 1999). Our new results suggest that GRC is a mechanosensitive channel and may be involved in the pathogenesis of myocyte degeneration caused by DGC disruption.

Results

GRC expression in normal and dystrophic striated muscles

We cloned Ca^{2+}-permeable cation channels structurally related to a subfamily of TRP channels, VR1 (Caterina et al., 1997), GRC, and a stretch-inhibitable channel (Suzuki et al., 1999), by PCR using degenerate primers for their conserved amino acid sequences. Out of 13 DNA fragments isolated from mouse heart total RNA, 12 contained the same sequence as that of GRC. Furthermore, screening of a mouse

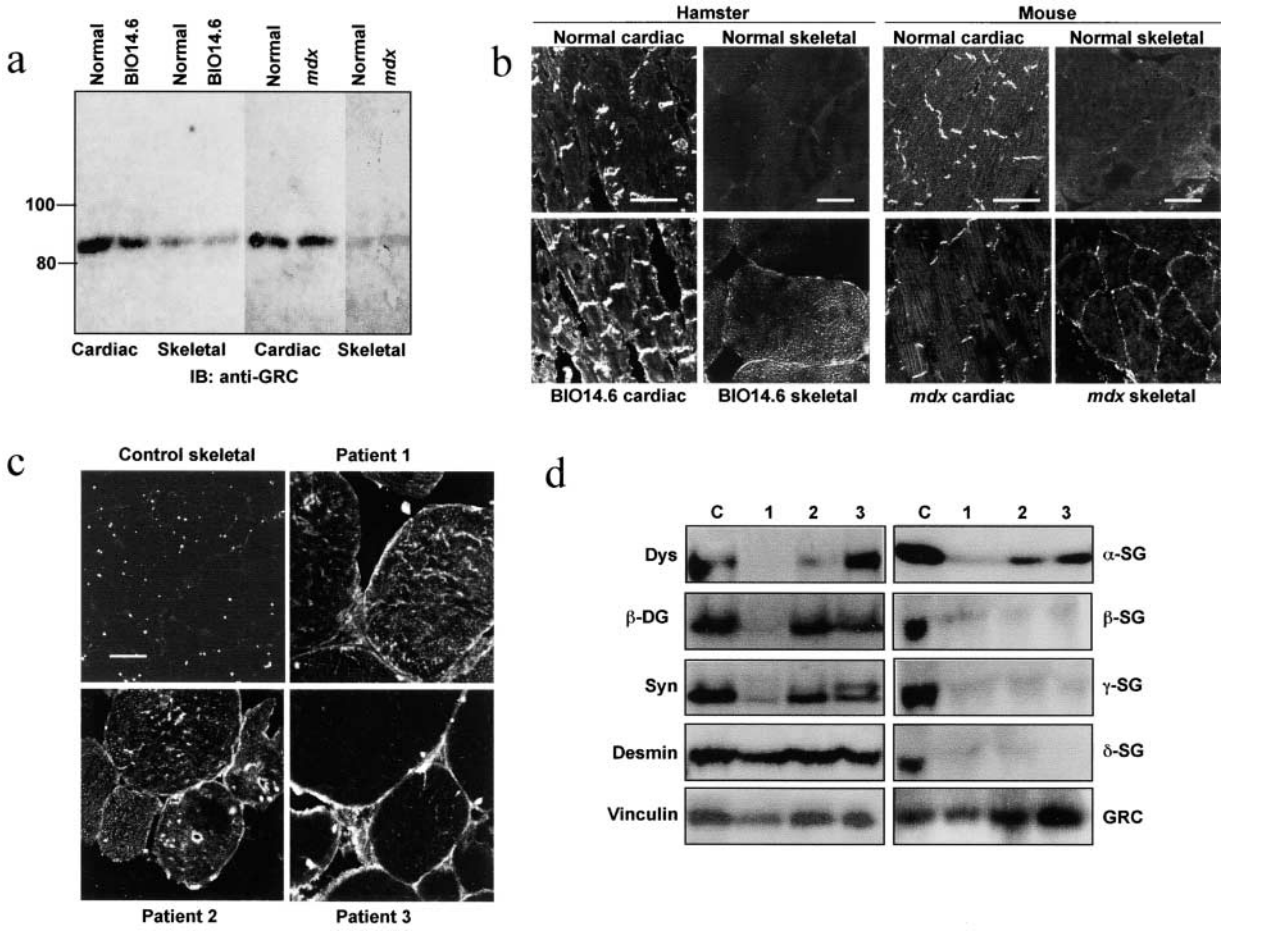

Figure 1. **Expression of GRC in dystrophic muscles.** (a) Contents of GRC protein in cardiac and skeletal muscles from BIO14.6 hamster, *mdx* mouse, and normal controls. Muscle homogenates (40 μg per lane) were subjected to immunoblot assay with anti-GRC. (b and c) Immunohistochemical localization of GRC in frozen sections of cardiac and skeletal muscles from normal and dystrophic animals and skeletal muscles from dystrophic patients and a nondystrophic control. Bars, 50 μm. (d) Immunoblot analysis of skeletal muscle homogenates from dystrophic patients and a nondystrophic control using antibodies against the indicated proteins. Samples correspond to those in c. Dys, dystrophin; SG, sarcoglycan; DG, dystroglycan; Syn, syntrophin.

cDNA library with the PCR product under low stringency conditions did not permit isolation of other clones related to TRP channels. Thus, among its homologues, GRC appears to be the predominant protein expressed in the heart.

We examined the expression of GRC protein in striated muscles of hamster and mouse. In an immunoblot assay, the 85-kD GRC protein was ~10-fold more abundant in cardiac than in skeletal muscle (Fig. 1 a). Immunohistochemical analysis of cardiac muscle revealed that GRC expression was prominent in the intercalated disc, but much less so in peripheral sarcolemma and the cell interior (Fig. 1 b). In skeletal myocytes, GRC was localized diffusely in the cell interior, with trace levels in the sarcolemma. Intriguingly, GRC in the peripheral sarcolemma was significantly elevated in cardiac and skeletal muscles of BIO14.6 hamsters and skeletal muscle of *mdx* mice compared with their normal counterparts (Fig. 1 b), although the GRC content did not differ markedly between normal and dystrophic muscles (Fig. 1 a). In *mdx* cardiac muscle, the sarcolemmal GRC was not elevated, which may be compatible with minimal dystrophic changes in the heart of this model (Torres and Duchen, 1987).

Anti-GRC staining of the sarcolemma was also much increased in skeletal muscles from myopathic patients with abnormal DGC. Patient 1 had Becker muscular dystrophy due to deletion of exons 47 and 48 of the dystrophin gene, and exhibited reduced expression of most components of the DGC (Fig. 1 d), although an antidystrophin COOH terminus antibody, Dys-2, was able to stain the sarcolemma (unpublished data). Patients 2 and 3 were diagnosed as having limb-girdle muscular dystrophy, and exhibited markedly reduced expression of β-, γ-, and δ-SGs; other DGC components, including α-sarcoglycan, were relatively well retained, except for dystrophin in Patient 2 (Fig. 1 d).

Properties of myotubes prepared from BIO14.6 hamster or *mdx* mouse

As in adult skeletal muscle, GRC expression was increased in the sarcolemma of cultured myotubes prepared from BIO14.6 hamster or *mdx* mouse, whereas it was present mostly in the interior of normal myotubes (Fig. 2 a). In the latter, GRC shifted its location from the cell interior to the sarcolemma in response to 10 ng/ml IGF-1 (Fig. 2 b) or

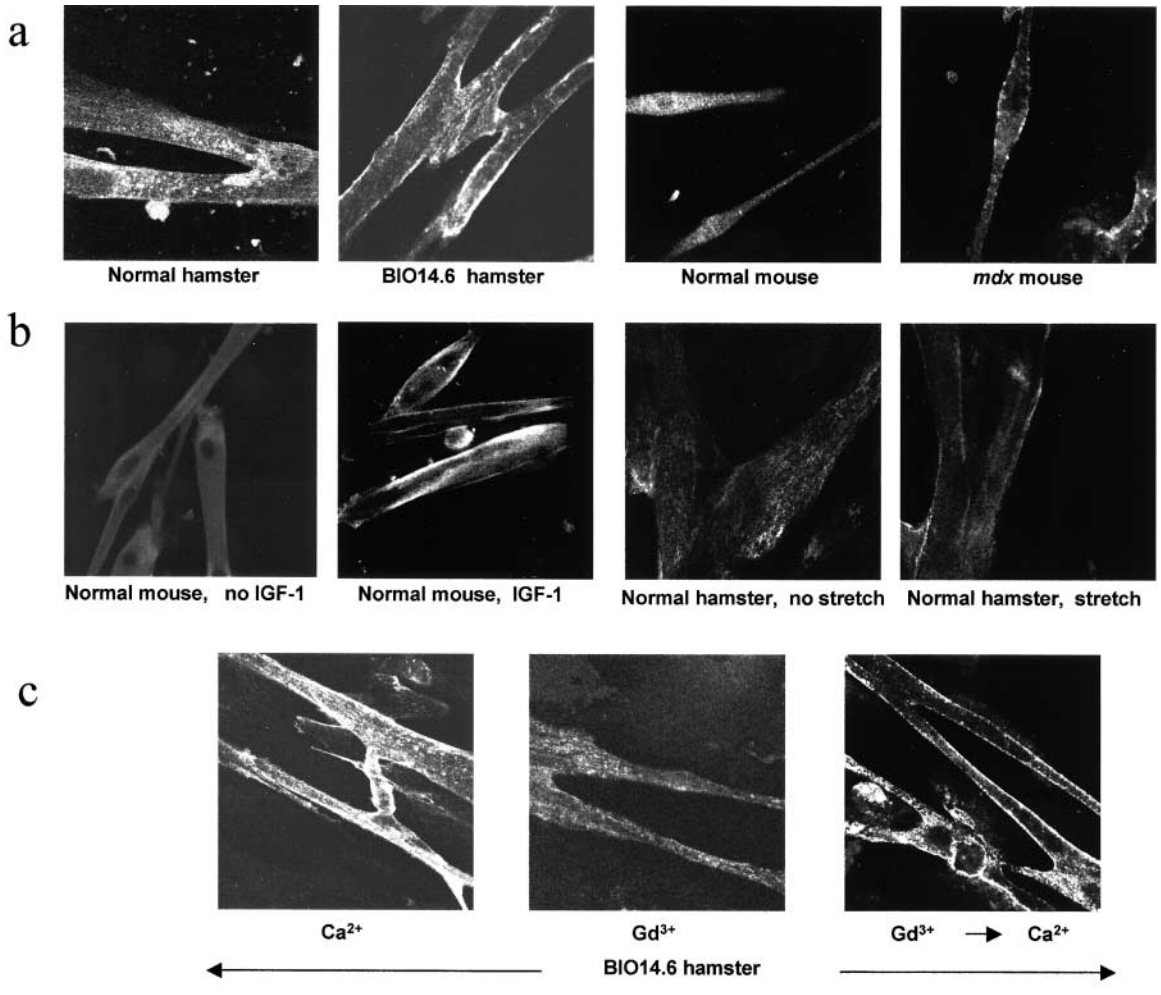

Figure 2. **GRC translocation in normal and dystrophic myotubes.** (a) Immunohistochemical localization of GRC protein in myotubes from BIO14.6 hamster and *mdx* mouse. (b) Effect of IGF-1 treatment or cyclic cell stretch on GRC translocation in normal mouse and hamster myotubes. (c) Ca^{2+}-induced shift of GRC localization in BIO14.6 myotubes. Myotubes initially placed in 2 mM Ca^{2+} were transferred to medium containing 0.5 mM Gd^{3+}, and 1 h later were transferred back to 2 mM Ca^{2+}.

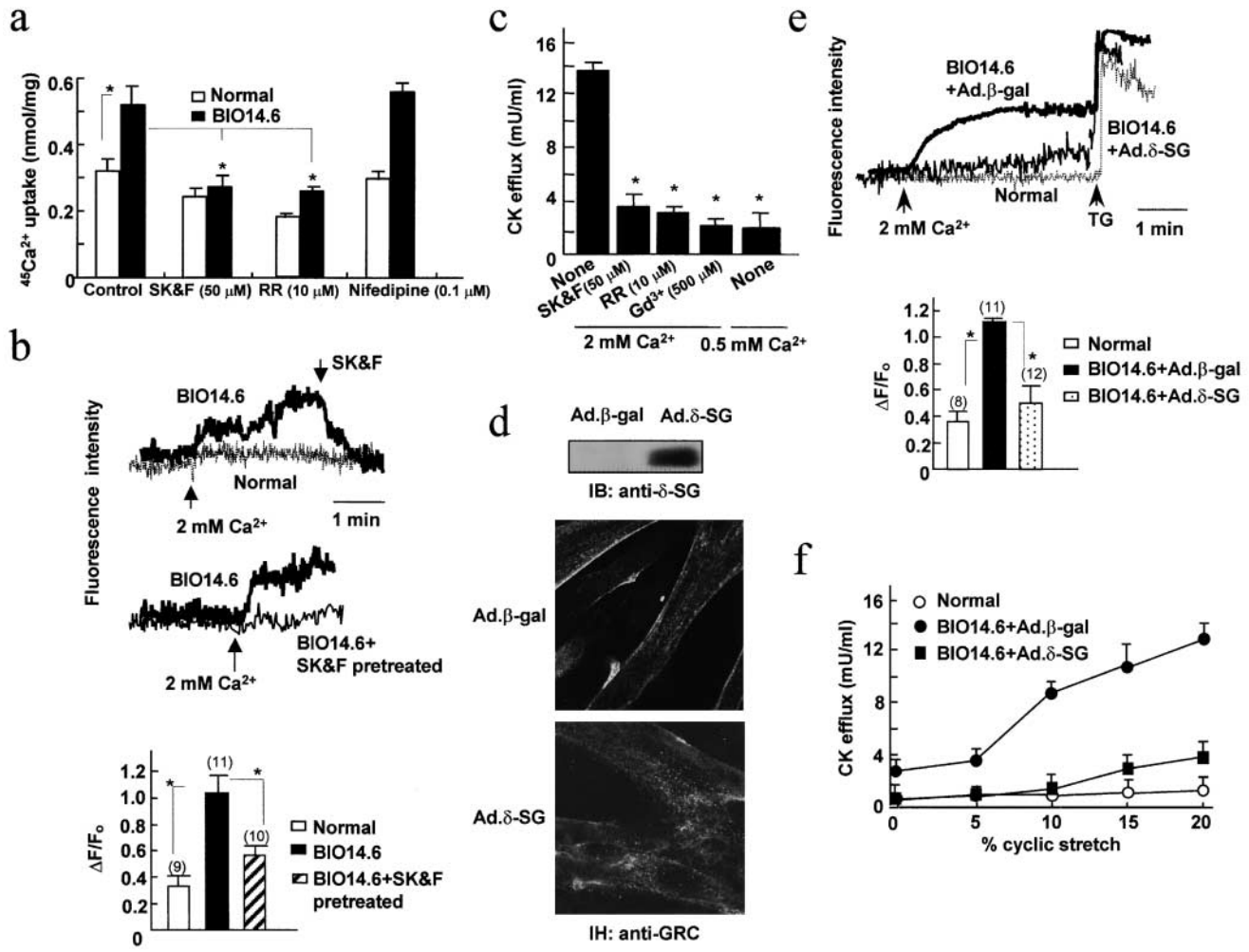

Figure 3. **Increased Ca^{2+} influx into and CK efflux from BIO14.6 myotubes and their correction by δ-SG gene transfer.** (a) $^{45}Ca^{2+}$ uptake into normal or BIO14.6 myotubes measured under resting conditions with or without SK&F96365 (SK&F), ruthenium red (RR), or Nifedipine. The Gd^{3+}-inhibitable fractions are shown. (b) External Ca^{2+}-induced changes in fluo-4 fluorescence in normal or BIO14.6 myotubes. The bar graph shows the maximal increments of fluorescence in myotubes pretreated with or without 50 μM SK&F96365. $\Delta F/F_0$ is the ratio between the fluorescence increment and the fluorescence before Ca^{2+} addition. Numbers in parentheses correspond to the number of cells studied. (c) CK efflux from BIO14.6 myotubes subjected to cyclic stretch under indicated conditions. (d) Immunoblot assay and immunohistochemistry (IH) of BIO14.6 myotubes infected with Ad.β-gal or Ad.δ-SG. (e and f) External Ca^{2+}-induced changes in fluo-4 fluorescence and cyclic stretch–induced CK efflux in BIO14.6 myotubes insfected with Ad.β-gal or Ad.δ-SG. TG, thapsigargin (1 μM). Other conditions were similar to b and c. In these panels, error bars show means ± SD and asterisks show $P < 0.05$.

10% FCS, as is the case in CHO cells (see Fig. 5 a; Kanzaki et al., 1999). GRC translocation also occurred when we subjected normal hamster myotubes to a cyclic stretch of 20% elongation for 15 min in 2 mM Ca^{2+} (Fig. 2 b). However, IGF-1– or stretch-induced GRC translocation did not occur in 0.5 mM Gd^{3+}. Interestingly, when we placed BIO14.6 myotubes in Gd^{3+}-containing medium, a slow but pronounced reduction in sarcolemmal GRC occurred (Fig. 2 c). Re-exposure of BIO myotubes to 2 mM Ca^{2+} resulted in the reappearance of GRC in the sarcolemma within 15 min. Unlike translocation induced by IGF-1 (Kanzaki et al., 1999), PI-3 kinase inhibitors (wortmannin or LY294002) did not inhibit this Ca^{2+}-induced translocation. Thus, Ca^{2+} seems to be a primary regulator of GRC translocation.

We also examined Ca^{2+} influx into resting hamster myotubes. In BIO14.6 myotubes, Gd^{3+}-sensitive $^{45}Ca^{2+}$ uptake was significantly greater compared with the controls and was markedly suppressed by ruthenium red or SK&F96365, but not by nifedipine (Fig. 3 a). On the other hand, when we elevated the external Ca^{2+} acutely from 0.5 to 2 mM, $[Ca^{2+}]_i$, as monitored by the fluo-4 fluorescence, increased significantly in BIO14.6 myotubes. SK&F96365 (Fig. 3 b), but not nifedipine (0.1 μM; unpublished data), inhibited the increase. In normal myotubes, 2 mM of external Ca^{2+} induced little change in fluo-4 fluorescence (Fig. 3 b). Of note, we obtained similar results when $[Ca^{2+}]_i$ was monitored using the ratiometric dye fura-2 in place of fluo-4.

The efflux of creatine phosphokinase (CK) from myotube cytoplasm can be regarded as an indicator of myocyte damage. When we applied a cyclic cell stretch of 20% elongation for 1 h in 2 mM Ca^{2+}, BIO14.6 myotubes released a high level of CK (~30% of the total cell activity). Normal myotubes released little CK activity, although the total cell activity of normal and myopathic myotubes did not differ. Prior

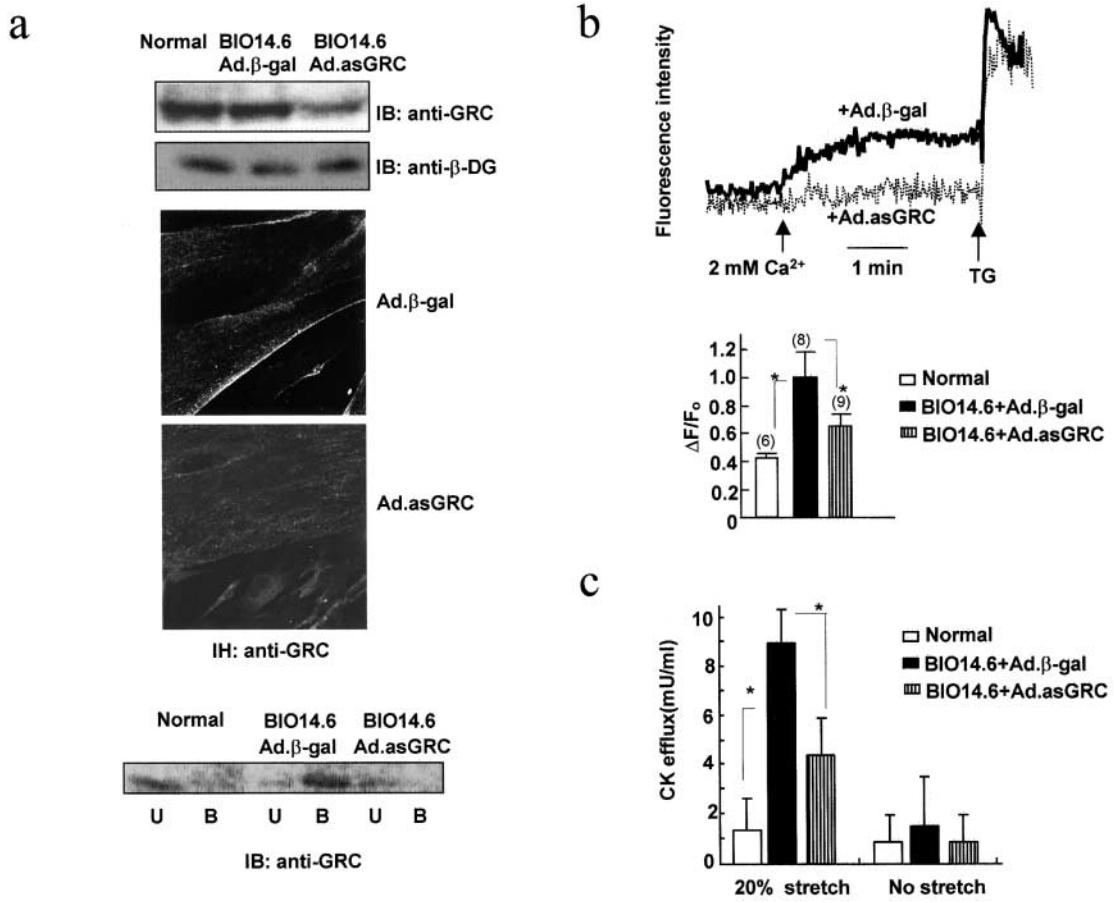

Figure 4. **Effect of GRC antisense expression on BIO14.6 myotubes.** (a) Immunoblot assay for GRC and β-dystroglycan (β-DG; top) and GRC immunohistochemistry (middle) of BIO14.6 myotubes infected with Ad.β-gal or Ad-antisense–GRC cDNA (Ad.asGRC). Cell surface GRC levels were estimated by labeling antisense-treated or nontreated myotubes with NHS-biotin and by further analyzing streptavidin agarose-bound (B) and -unbound (U) fractions by immunoblot assay with anti-GRC (bottom). (b and c) External Ca^{2+}-induced changes in fluo-4 fluorescence and cyclic stretch-induced CK efflux from antisense-treated or nontreated myotubes. Other conditions were the same as those in Fig. 3 (b and c). Error bars show means ± SD and asterisks show $P < 0.05$.

treatment of cells with SK&F96365 or ruthenium red, reducing the external Ca^{2+} to 0.5 mM, or adding 0.5 mM Ga^{3+} markedly suppressed CK efflux from BIO14.6 myotubes (Fig. 3 c).

It should be noted that infection of the cells with an adenoviral vector carrying δ-SG cDNA corrected all the above abnormalities observed in BIO14.6 myotubes. Immunoblot and immunohistochemical analyses revealed that elevated sarcolemmal GRC levels were down-regulated in infected myotubes, whereas δ-SG and other DGC components were expressed as in normal myotubes (Fig. 3 d; unpublished data). Similarly, δ-SG cDNA-infection of BIO14.6 myotubes significantly suppressed the rise in fluo-4 fluorescence in response to external Ca^{2+} addition (Fig. 3 e) and stretch-induced CK efflux (Fig. 3 f).

We further examined whether GRC was involved in the external Ca^{2+}-induced increase in $[Ca^{2+}]_i$ or stretch-induced CK efflux in BIO14.6 myotubes. Infection of BIO myotubes with GRC antisense cDNA reduced the GRC protein to 30–40% of the original level (Fig. 4 a). Immunostaining with anti-GRC revealed markedly reduced expression of GRC in the sarcolemma of treated myotubes, although some still remained in the cell interior. Consistent with this finding, a low level of GRC protein was labeled with membrane-impermeable *N*-hydroxysuccinimido-biotin (NHS-biotin) applied from the outside. Importantly, both the rise in $[Ca^{2+}]_i$ and CK efflux during a 1-h stretch were significantly suppressed in antisense DNA-treated BIO14.6 myotubes (Fig. 4, b and c), strongly suggesting the involvement of GRC in the observed abnormalities.

Properties of CHO cells expressing exogenous GRC

We used serum-starved CHO cells lacking endogenous GRC to study the functional consequences of exogenous GRC surface expression. GRC was predominantly localized in the cell interior at rest, moving to the cell surface on 10% FCS addition (Fig. 5 a). IGF-I (10 ng/ml) or FCS induced $[Ca^{2+}]_i$ to rise slowly in these cells. No rise was observed in the presence of 50 μM Gd^{3+} or 50 μM SK&F96365, which is consistent with previous papers (Kanzaki et al., 1999; Boels et al., 2001). Cyclic stretch of 10% elongation significantly enhanced $^{45}Ca^{2+}$ uptake by GRC-transfected CHO cells, but not by nontransfected cells (Fig. 5 b). It is noteworthy that $^{45}Ca^{2+}$ uptake was significantly greater in GRC-transfected cells than in nontransfected ones, even in the absence of stretch. Consistent with these findings, a short stretch in 2 mM Ca^{2+} in-

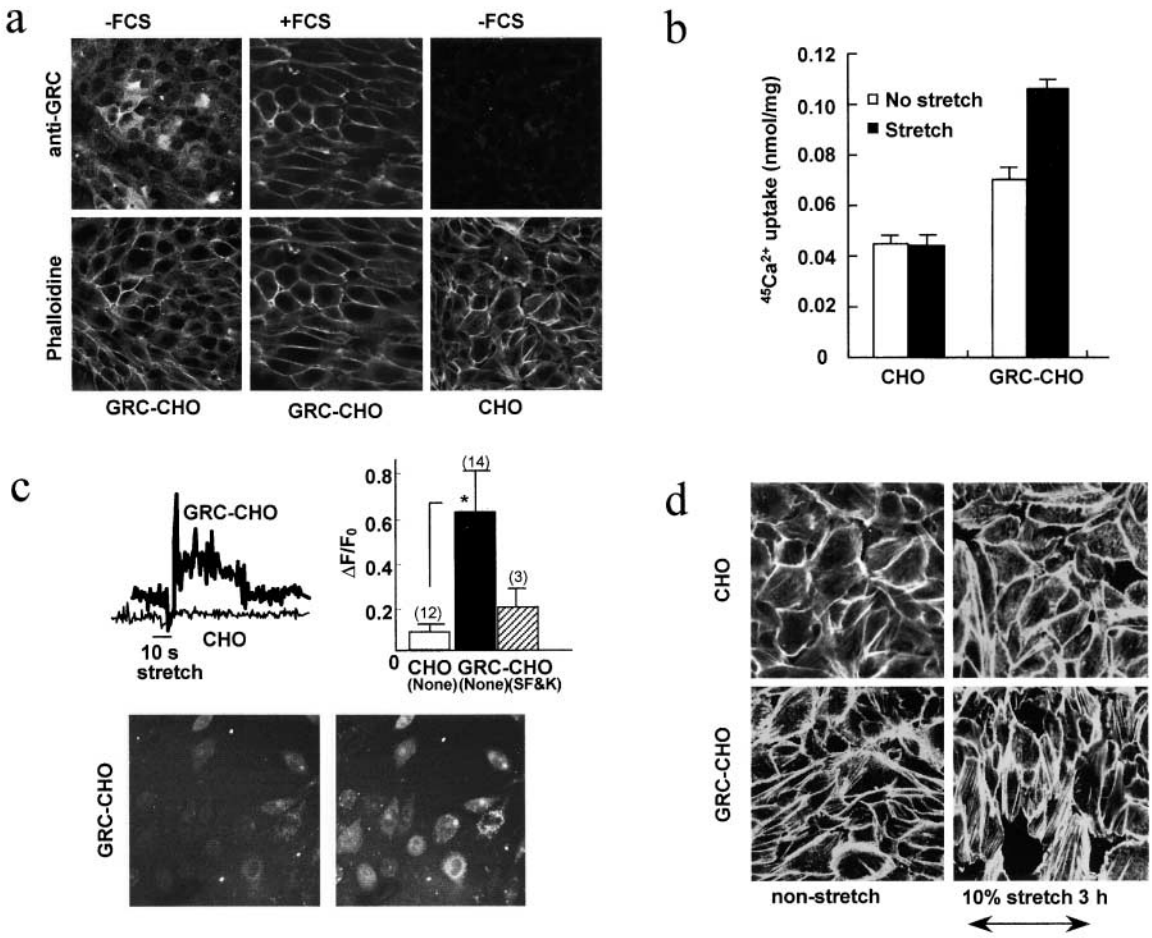

Figure 5. **Characterization of CHO cells expressing GRC.** (a) Effect of FCS on GRC localization in CHO cells serum-starved for 24 h. Cells were stained with anti-GRC or rhodamine-phalloidin. (b) Gd^{3+}-inhibitable $^{45}Ca^{2+}$ uptake into GRC-transfected or nontransfected cells measured for 5 min with cyclic stretch applied for 3 min starting from the end of the first min. (c) Stretch–induced changes in $[Ca^{2+}]_i$ as monitored by the fluo-4 fluorescence. The maximal increments of fluorescence are shown in the bar graph (mean ± SD). Microscopic fields before and after stretch showing low and elevated levels of fluorescence in GRC-expressing cells (bottom). Data represent a typical result from four similar experiments. (d) Effect of uniaxial cyclic stretch on the cell orienting response. Rhodamine-phalloidin–stained images of nonstretched and stretched cells are shown. In b and c, error bars show means ± SD and asterisks show $P < 0.05$.

duced a transient rise in fluo-4 fluorescence only in GRC-transfected cells cultured on an elastic silicone membrane, which was inhibited by 50 μM SK&F96365 (Fig. 5 c). These results suggest that stretch enhanced Ca^{2+} influx via GRC.

Uniaxial cyclic stretch has been shown to induce human umbilical vein endothelial cells to align perpendicularly to the axis of stretch (Shirinsky et al., 1989). When we subjected GRC-transfected CHO cells to 10% uniaxial stretch at 1 Hz for 3 h, we observed enhanced stress fiber formation as well as a shift in the cell orientation transverse to the strain direction (Fig. 5 d). This orienting response, which we observed only in GRC-transfected cells, became noticeable after ∼90 min; it did not occur in the presence of 50 μM Gd^{3+} (unpublished data). Thus, it appears that stretch-dependent Ca^{2+} influx via GRC is likely to cause cytoskeletal reorganization in transfected CHO cells.

Transgenic mouse model of cardiac GRC overexpression

To examine the pathological consequences of GRC expression in vivo, we generated transgenic mice overexpressing GRC in cardiac muscle (Fig. 6). Out of the four female and seven male founders (F0s) obtained, three females died peripartum during their first pregnancy. These three F0s expressed the GRC protein at a level 10-fold of that of nontransgenic controls, and had markedly elevated sarcolemmal GRC (Fig. 6 a). Two of the males had two- to threefold higher levels of GRC protein, as well as increased sarcolemmal GRC. These male F0s and a sterile female exhibited prominent anasarca at the age of ∼180 d when we demonstrated left ventricular dilation and compromised systolic performance by M-mode echocardiography. Other male founders exhibited normal levels of GRC protein and normal cardiac function, although they had at least a single copy of the transgene.

The female F0s that died peripartum developed globally enlarged hearts due to size increases of all four chambers (Fig. 6 a). Also, the left ventricular wall and the septum were mildly thickened compared with the nontransgenic controls. Under light microscopy, the hearts exhibited a disorganized myocyte arrangement, a pronounced increase in nonmyo-

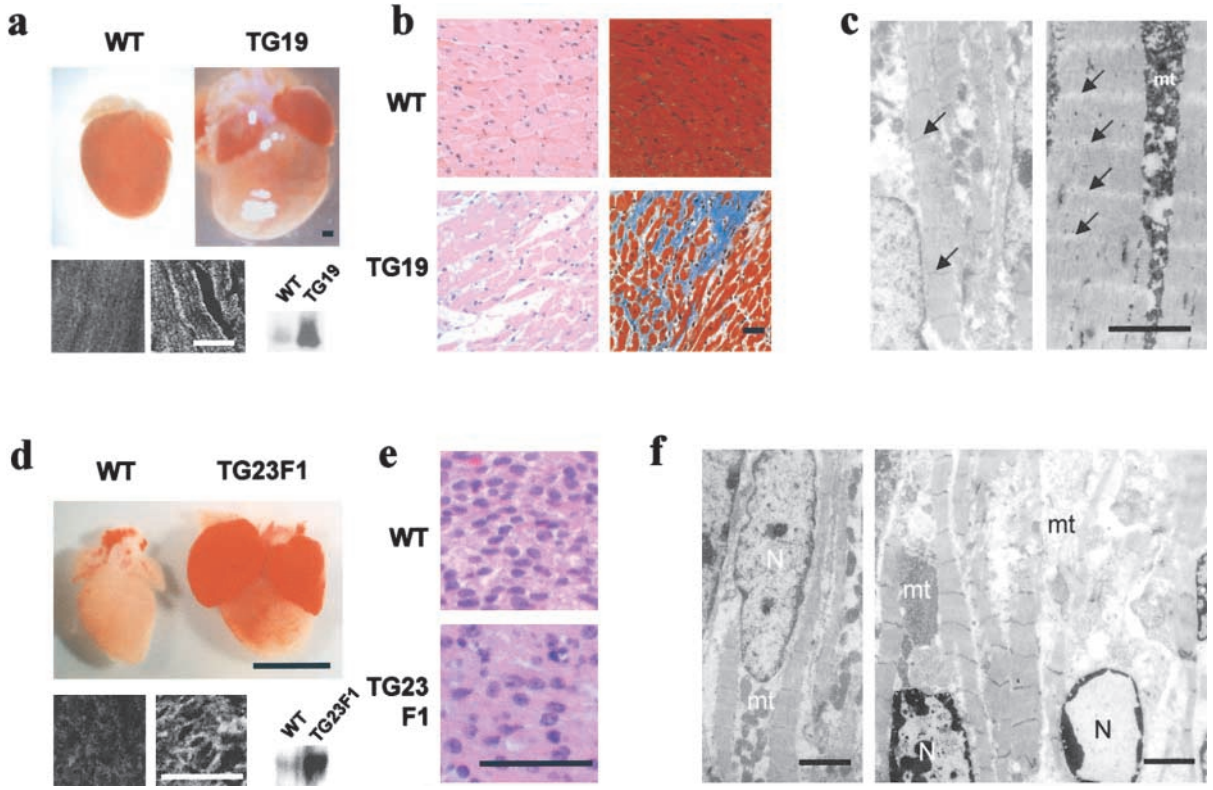

Figure 6. **Histological analysis of GRC overexpressing transgenic hearts.** (a) Hearts were excised from 120-d-old nontransgenic (WT) and transgenic (TG19 founder line) mice. (heart) Bar, 1 mm. (bottom) Immunoblot and immunohistochemical analyses of GRC protein in WT and TG19 ventricles. For the latter analysis, paraffin sections were used (left, WT; right, TG19). (b) Sections of heart from WT and TG19 mice stained with hematoxylin and eosin (left) or Masson's trichrome (right). (c) Ultrastructural analysis of WT (left) and TG19 (right) ventricles. Z-lines are lost in TG19 (arrows). (d) Hearts excised from 1-d-old nontransgenic (WT) and transgenic (TG23F1) mice. (heart) Bar, 1 mm. (bottom) Immunoblot and immunohistochemical analyses of GRC protein in WT and TG23F1 ventricles. For the latter analysis, paraffin sections were used (left, WT; right, TG23F1). (e) Sections of ventricles from WT and TG23F1 mice stained with hematoxylin and eosin. (f) Ultrastructural analysis of WT (left) and TG23F1 (right) ventricles. Bars: (light microscopy) 50 μm; (EM) 2 μm. mt and N denote mitochondria and nuclei, respectively.

cyte space, and prominent interstitial fibrosis (Fig. 6 b). A prominent feature revealed by EM was the disappearance of Z bands in the myofibrils, with apparently preserved myofilament alignment (Fig. 6 c). Mitochondria were also markedly swollen.

The F1 offspring generated by mating a GRC-overexpressing male F0 (TG23) with normal female mice all died perinatally. GRC protein in the hearts of these F1 mice was threefold higher than that of their nontransgenic littermates, and its level in the sarcolemma was also elevated (Fig. 6 d). The hearts showed global enlargement affecting all four chambers, and both atrial chambers were filled with organized thrombi (Fig. 6 d). Although few histological abnormalities were detected by light microscopy, ultrastructural analysis of these F1 hearts often revealed partial disruption of myofibrils along with irregularly spaced or markedly shortened sarcomeres, perinuclear chromatin condensation, and swollen mitochondria. In contrast, F1 offspring from male F0s other than TG23 possessed normal levels of GRC and few cardiac abnormalities were evident.

All of these morphological changes in female F0 and F1 mice were very similar to those seen in damaged cardiac muscle under conditions in which cytosolic Ca^{2+} in myocytes is greatly elevated (Reimer and Jenning, 1986). Consistent with these alterations in cell structure, we found that a large population of ventricular myocytes from GRC transgenic mice, i.e., ~40% (249 TUNEL-positive cells in 608 myocytes) in the TG19 female F0 and 18% (115 TUNEL-positive cells in 628 myocytes) in the TG23 F1 mice, stained positive in a TUNEL assay, suggesting the occurrence of extensive apoptosis. Together, these results suggest that a close association exists between the level of GRC expression versus myocyte damage and loss of in vivo cardiac function in GRC transgenic mice.

Discussion

Disruption of the DGC predisposes striated muscle cells to progressive degeneration and contraction-induced damage. Although the mechanism by which DGC disruption leads to expression of the dystrophic phenotype has yet to be clarified, accumulating evidence suggests that the muscle pathology involves abnormal cell Ca^{2+} handling. Our findings provide evidence that abnormal Ca^{2+} influx is a key early event in the pathogenesis of muscle degeneration caused by DGC disruption.

Chronic elevation of $[Ca^{2+}]$ in the cytoplasm and other intracellular compartments has been reported in the cases of

mdx skeletal fibers and cultured myotubes from dystrophin-deficient DMD patients and *mdx* mice (Fong et al., 1990; Brown and Lucy, 1997: Mallouk et al., 2000; Alderton and Steinhardt, 2000b; Robert et al., 2001). This could be due to increased Ca^{2+}-specific leak channel or mechanosensitive cation channel basal activity, as has been demonstrated in cultured myotubes from DMD patients, *mdx* mice, and δ-SG–deficient BIO14.6 hamsters (Fong et al., 1990; Franco-Obregon and Lansman, 1994; Alderton and Steinhardt, 2000b; Nakamura et al., 2001; Vandebrouck et al., 2001). In these dystrophic muscle preparations, elevated $[Ca^{2+}]_i$ has been causally linked to a greater rate of protein degradation catalyzed by Ca^{2+}-dependent protease calpain (Turner et al., 1988; MacLennan et al., 1991; Spencer et al., 1995; Alderton and Steinhardt, 2000a), which with concurrent myocyte contractile activity would cause physical damage to the sarcolemma, leading to leakage of cytosolic enzymes such as CK. Physical cell damage was indeed demonstrated in vitro in isolated *mdx* fibers and in vivo in the muscle of dystrophic patients (Mokri and Engel, 1975; Menke and Jockusch, 1991; Petrof et al., 1993). Dystrophic patients and animal models also show consistently elevated CK levels in their serum, although this is not always closely correlated with clinical symptoms (Brown and Lucy, 1997).

In δ-SG–deficient BIO14.6 myotubes, we detected elevated basal activity of a nifedipine-insensitive, ruthenium red– or SK&F96365-inhibitable Ca^{2+} influx as monitored by an external Ca^{2+}-induced rise of the intracellular Ca^{2+}-sensitive dye fluorescence or $^{45}Ca^{2+}$ uptake (Fig. 3, a and b). We also observed efflux of high CK activity from BIO14.6 myotubes in response to cyclic stretch under conditions in which little efflux occurred from normal myotubes (Fig. 3, c and f). The CK efflux was suppressed by the Ca^{2+} influx inhibitors Gd^{3+}, ruthenium red, and SK&F96365 (Fig. 3 c) or pretreatment of myotubes with the calpain inhibitor E64 (Sampaolesi et al., 2001; unpublished data). Furthermore, adenoviral transfer of δ-SG cDNA to BIO14.6 myotubes caused significant reductions in resting Ca^{2+} influx and stretch-induced CK efflux (Fig. 3, d–f). Hence, BIO14.6 myotubes seem to retain the original phenotypes of dystrophic muscle. We have observed similar cell abnormalities in myotubes prepared from the rat L6 myoblasts or rat skeletal muscle that were rendered deficient of sarcoglycans by treatment with antisense oligonucleotides (Sampaolesi et al., 2001).

GRC is a Ca^{2+}-permeable nonselective cation channel belonging to the TRP channel family, which translocates from the cell interior to the surface in response to growth factors (Kanzaki et al., 1999; Boels et al., 2001). GRC is normally expressed in adult striated muscles, with low expression in the sarcolemma except in cardiac intercalated discs (Fig. 1). In normal hamster myotubes, sarcolemmal GRC expression was transiently elevated only on the first day of cell fusion, whereas in BIO14.6 myotubes, this initial expression continued (Fig. 2; unpublished data). Intriguingly, in normal myotubes, cell stretch increased sarcolemmal GRC expression, which required entry of external Ca^{2+} (Fig. 2, b and c). This triggering Ca^{2+} could have entered via a low level of GRC initially present in the sarcolemma. However, little is known as to what initially triggers the surface translocation of GRC during the formation of myotubes. The situation was somewhat similar in the case of GRC-transfected CHO cells; an applied stretch enhanced Ca^{2+} influx into the transfected cells, which was blocked by Gd^{3+}, ruthenium red, or SK&F96365 (Fig. 5; Results). Although these inhibitors are not specific for GRC (Boels et al., 2001), the enhanced Ca^{2+} influx was not observed in cells without GRC. Furthermore, GRC-transfected CHO cells exhibited changes in cell orientation and cytoskeletal organization in response to a relatively long stretch, which appears to be mediated by Gd^{3+}-inhibitable Ca^{2+} influx via GRC (Fig. 5).

Importantly, sarcolemmal GRC was elevated in skeletal muscles from human patients with muscular dystrophy, BIO14.6 hamsters, and *mdx* mice (Fig. 1, b and c). It also increased in the sarcolemma of BIO14.6 cardiac muscle, but not in *mdx* cardiac muscle, in which little dystrophic damage occurs (Torres and Duchen, 1987). In BIO14.6 myotubes, re-expression of δ-SG protein by gene transfer markedly reduced sarcolemmal GRC, abnormal Ca^{2+} influx, and stretch-induced CK efflux (Fig. 3, d–f). Similarly, reduction of sarcolemmal GRC by treatment with GRC antisense cDNA decreased Ca^{2+} influx and CK efflux in BIO14.6 myotubes (Fig. 4). These results, together with the functional properties of GRC discussed in the preceding paragraph, strongly suggest that the sarcolemmal GRC level and expression of dystrophic phenotypes are causally linked. A recent paper has implicated TRPC subfamily members of TRP channels in voltage-independent Ca^{2+} channel activity in *mdx* fibers, based on inhibition of the latter by antisense oligonucleotides with sequences conserved in all TRPC channel isoforms (Vandebrouck et al., 2002). Although GRC belongs to a different subfamily, it could also be an antisense target.

The in vivo pathological consequence of GRC expression in the sarcolemma may be inferred from cardiac abnormalities observed in GRC transgenic mice (Fig. 6). Female founders died peripartum during their first pregnancy, whereas F1 mice from TG23 line all died perinatally. These mice exhibited globally enlarged hearts and extensive myocyte damage, with strong indications of apoptosis (Results). Similar cell abnormalities are typically seen in Ca^{2+}-overloaded cardiac muscle (Reimer and Jenning, 1986) and, though not as extensively, in some necrotic areas of dystrophic skeletal muscles from DMD patients and *mdx* mice (Cullen and Fulthorpe, 1975; Cullen and Jaros, 1988). Furthermore, the results obtained with these transgenics suggest that there is a correlation between GRC expression, myocyte damage, and the loss of cardiac function (Fig. 6; Results). It seems likely that elevated levels of sarcolemmal GRC result in greater Ca^{2+} influx in response to mechanical stress in the cardiac chamber walls, causing further mobilization of GRC on the cell surface, thereby exacerbating Ca^{2+} overloading and the resultant cell damage.

GRC was originally identified as a Ca^{2+}-permeable cation channel activated by IGF-1 and other growth factors (Kanzaki et al., 1999). IGF-1 is thought to be an important mediator of anabolic pathways in skeletal myocytes, playing a critical role in myocyte proliferation, differentiation, and regeneration after injury (Stewart and Rotwein, 1996). Skeletal muscle-specific expression of IGF-1 in transgenic *mdx*

mice has been shown to counter muscle decline by promoting hypertrophy and hyperplasia of myocytes while preventing apoptosis (Barton et al., 2002). Furthermore, it has been reported that IGF-1 improves cardiac performance in experimental cardiac failure (Duerr et al., 1995). However, long-term exposure of cardiac muscle to IGF-1 in a transgenic mouse model resulted in decreased systolic performance and marked interstitial fibrosis, suggesting the potentially deleterious effects of high levels of IGF-1 on the muscle function (Delaughter et al., 1999). IGF-1 most likely activates multiple signaling pathways in myocytes, with GRC being one of its downstream targets. However, how GRC is involved in the overall function of IGF-1 is currently unclear.

In summary, the data suggest that abnormal Ca^{2+} influx and the resultant cell damage occur via GRC in δ-SG–deficient hamster muscle. GRC is likely to function in a similar manner in dystrophin-deficient humans and mice. Because mechanical stress enhances GRC-mediated Ca^{2+} influx, it is important to examine whether GRC also plays a critical role in the initiation or progression of other skeletal and/or cardiac myopathies of genetic or nongenetic origin.

Materials and methods

Preparation of tissues and primary myotube culture

We used male BIO14.6 hamsters (SLC Japan; Nakamura et al., 2001) and male *mdx* mice (Jackson Laboratories) 5–8 wk old and age-matched controls. We obtained biopsy samples of the vastus lateralis muscle from patients after their informed consent. We prepared satellite cells from the gastrocunemius muscle of hamsters or mice by enzymatic dissociation as described by Rando and Blau (1994), except that the initial enzyme cocktail for cell dissociation contained 0.5 mM $CaCl_2$, instead of 2.5 mM, and Ham's F12 medium supplemented with 20% FCS, 2.5 ng/ml bFGF (Promega), and 1% chick embryo extract (GIBCO BRL) was used for hamster myoblasts. After enrichment of the myoblasts by several preplatings, we changed the medium to DME containing 2% horse serum to induce myotube formation. We performed experiments using myotubes cultured for 2–4 d (for hamster) and >10 d (for mouse) after the start of fusion.

cDNA cloning and expression in cells

For cloning of GRC, we amplified cDNAs prepared from mouse heart total RNA by PCR using degenerated forward and reverse primers corresponding to aa 596–601 and aa 698–703 of mouse GRC (Kanzaki et al., 1999), respectively, which are conserved in rat VR1 (Caterina et al., 1997) and a mouse stretch–inhibitable channel (Suzuki et al., 1999). Amplification conditions consisted of incubation at 94°C for 30 s, 52°C for 30 s, and 72°C for 30 s for a total of 25 cycles. Subsequent low stringency screening (hybridization, 30% formamide at 48°C; washing, 2× SSC and 0.1% SDS at 55°C) of a mouse heart cDNA library (Stratagene) with the PCR product from GRC permitted the isolation of many clones, but did not produce any related to TRP channels except GRC. We tagged GRC cDNA with a hemagglutinin epitope and subcloned it into the pIRES expression vector (Invitrogen), which we transfected into CHO-K1 cells and selected with puromycin.

For adenoviral gene transfer, we ligated full-length cDNA of hamster δ-SG or β-galactosidase (β-gal), or full-length antisense cDNA of mouse GRC into the Adeno-X™ viral vector (CLONTECH Laboratories, Inc.) according to the manufacturer's protocol. We infected 1-d-old myotubes in differentiated medium with adenoviruses at a multiplicity of infection of 5–10 viral particles per cell for 24 h and cultured them for an additional 36–48 h.

Generation of transgenic mice

We constructed the transgene by inserting full-length mouse GRC cDNA between the mouse α-MHC promoter and the SV40 polyadenylation sequence of the plasmid (provided by Dr. J. Robbins, The Children's Hospital Research Foundation, Cincinnati, OH). We microinjected the transgene into the male pronucleus of fertilized eggs from C57BL/6 mouse, which was implanted into pseudopregnant foster mothers. We identified positive transgenic mice either by Southern blotting or PCR detection of the transgene. For PCR detection of the transgene, sense and antisense primers specific for the α-MHC gene and a coding region of mouse GRC were used. Transgenic founders were mated with wild-type C57BL/6 mice to generate F1 offspring.

Examination of histology, ultrastructure, and TUNEL-positive cells

We fixed hearts of transgenic mice in PBS containing 10% formalin and embedded them in paraffin. We stained serial 5-μm sections of samples from the free wall of the left ventricles with hematoxylin/eosin or Masson's trichrome to evaluate gross morphology and fibrosis. For ultrastructural analysis, we fixed and dehydrated samples according to the standard method, and viewed the sections through a transmission microscope (model H7000; Hitachi). We assayed TUNEL-positive cells using an apoptosis detection kit (Takara Biomedical) essentially as described previously (Saito et al., 2000). The number of TUNEL-labeled nuclei was counted by observing specimens from the TG19 female F0 and three TG23 F1 mice and their normal controls with a light microscope (40× objective; Olympus). TUNEL-positive cells were <3% in normal mouse ventricles.

Antibodies, immunoblotting, and immunohistochemistry

We raised polyclonal anti-GRC or anti–δ-SG antibody by immunizing rabbits or chickens with GST fusion proteins containing aa 634–756 of mouse GRC protein or aa 1–32 of hamster δ-SG, respectively. We affinity-purified these antibodies as described previously (Bertrand et al., 1994). Other antibodies used were described previously (Iwata et al., 1996; Yoshida et al., 1998) or obtained commercially (antidystrophin NCL-Dys-1, -2, and -3; Novocastra Laboratories). We performed immunoblot and immunohistochemical analyses as described previously (Yoshida et al., 1998; Sampaolesi et al., 2001).

$^{45}Ca^{2+}$ uptake and $[Ca^{2+}]_i$ measurement

We measured $^{45}Ca^{2+}$ uptake into cells cultured on collagen I–coated 24-well dishes or silicon membranes at 37°C for 5 min in balanced salt solution (mM: 146 NaCl, 4 KCl, 2 $MgCl_2$, 1 $^{45}CaCl_2$, 10 glucose, 10 Hepes/Tris, pH 7.4, and 0.1% BSA) containing 0 or 0.5 mM $GdCl_3$ (Sampaolesi et al., 2001). The Gd^{3+}-inhibitable fraction of $^{45}Ca^{2+}$ uptake was calculated by subtracting the uptake in the presence of Gd^{3+} from that in its absence.

To monitor changes in $[Ca^{2+}]_i$, we loaded cells cultured on a cover glass with 4 μM fluo-4 acetoxymethyl ester at 37°C for 30 min in balanced salt solution containing 0.5 mM Ca^{2+}. We observed fluorescence signals from the cells at room temperature (~25°C) using a confocal microscope (model MRC-1024; Bio-Rad Laboratories) mounted on an microscope (model BX50WI; Olympus) with a plan-apochromat 60× water immersion lens. An argon laser was used to excite fluo4 at 488 nm. We acquired images at a rate of one image every second and used LaserSharp software (Bio-Rad Laboratories) to analyze single frames or the single cell–integrated signal density. In some experiments, we loaded cells with 2 μM fura-2 acetoxymethyl ester in place of fluo-4 acetoxymethyl ester and measured $[Ca^{2+}]_i$ by means of a ratiometric fluorescence method, using a fluorescence image processor (model Argus 50; Hamamatsu Photonics) mounted on an inverted microscope (40× objective; Nikon). The excitation wavelengths of 340 and 380 nm were alternated at 1 Hz, and the fluorescence light emitted at 510 nm was measured. The fluorescence ratio $R_{340/380}$ was calculated and $[Ca^{2+}]_i$ was determined using a K_d of 224 nM for the dissociation of fura-2–Ca^{2+} complex (Grynkiewicz et al., 1985).

Application of stretch to cells

We applied a uniaxial sinusoidal stretch of up to 120% to cells at 1 Hz and 25°C using a temperature-controlled stretching apparatus (model NS-300; SCHOLAR-TEC Co.) driven by a computer-controlled stepping motor, as described previously (Naruse et al., 1998). We cultured the cells in a silicon chamber with 400-μm-thick side walls and a 200-μm-thick transparent bottom coated with collagen I. In this way, uniform stretch was applied to most of cells cultured on the bottom (Naruse et al., 1998). To observe the effect of stretch on cell $[Ca^{2+}]_i$ response, the stretching apparatus was modified for use on a microscope, which allowed the silicone chamber to be placed on a confocal laser scanning microscope.

Surface labeling with NHS-biotin

We performed surface labeling of GRC protein in myotubes with membrane-impermeable NHS-biotin as described previously (Wakabayashi et al., 2000). In brief, we treated myotubes with 1 mM NHS-biotin for 30 min at room temperature, solubilized with the lysis buffer (1% Triton X-100, 150 mM NaCl, 20 mM Hepes/Tris, pH 7.4, 0.1% SDS, 1% sodium deoxy-

cholate, 1 mM benzamidine, 0.25 mM phenylmethylsulfonyl flouride, and 2.5 μg/ml aprotinin), and incubated for 1 h with streptavidin–agarose beads. After washing, the proteins were released from the beads by boiling in 3% SDS buffer and subjected to immunoblotting with anti-GRC.

Other procedures and materials

We determined CK activity in medium using an in vitro colorimetric assay kit (Wako Chemicals) according to the manufacturer's instruction (Sampaolesi et al., 2001). Protein concentration was measured using a bicinchoninic acid assay system (Pierce Chemical Co.) with BSA as a standard. Gadolinium chloride hexahydrate, IGF-1, and LY294002 were purchased from Sigma-Aldrich. Thapsigargin was obtained from Calbiochem. SK&F96365 was obtained from BIOMOL Research Laboratories, Inc., and ruthenium red was obtained from Wako Chemicals. NHS-biotin and streptavidin-conjugated agarose were purchased from Pierce Chemical Co. Fluo-4AM was purchased from Molecular Probes and fura-2AM was purchased from Dojin Chemicals. $^{45}CaCl_2$ was obtained from NEN Life Science Products.

Statistical analysis

Data are presented as means ± SD of three or four determinations unless otherwise stated. We used the *t* test to make comparisons between two groups. $P < 0.05$ was considered significant.

This work was supported by Special Coordination Funds from the Ministry of Education, Culture, Sports, Science and Technology of Japan and by a grant for Promotion of Fundamental Studies in Health Science from the Organization of Pharmaceutical Safety and Research. Y. Katanosaka is a domestic research fellow of the Japan Society for the Promotion of Science.

Submitted: 24 January 2003
Revised: 29 April 2003
Accepted: 29 April 2003

References

Alderton, J.M., and R.A. Steinhardt. 2000a. Calcium influx through calcium leak channels is responsible for the elevated levels of calcium-dependent proteolysis in dystrophic myotubes. *J. Biol. Chem.* 275:9452–9460.

Alderton, J.M., and R.A. Steinhardt. 2000b. How calcium influx through calcium leak channels is responsible for the elevated levels of calcium-dependent proteolysis in dystrophic myotubes. *Trends Cardiovasc Med.* 10:268–272.

Bajusz, E., F. Homburger, J.R. Baker, and P. Bogdonoff. 1969. Dissociation of factors influencing myocardial degeneration and generalized cardiocirculatory failure. *Ann. NY Acad. Sci.* 156:396–420.

Barton, E.R., L. Morris, A. Musarao, N. Rosenthal, and H.L. Sweeney. 2002. Muscle-specific expression of insulin-like growth factor 1 counters muscle decline in mdx mice. *J. Cell Biol.* 157:137–147.

Bertrand, B., S. Wakabayashi, S. Ikeda, J. Pouysségur, and M. Shigekawa. 1994. The Na^+/H^+ exchanger isoform 1 (NHE1) is a novel member of the calmodulin-binding proteins. Identification and characterization of calmodulin-binding sites. *J. Biol. Chem.* 269:13703–13709.

Boels, K., G. Glassmeier, D. Herrmann, I.B. Riedel, W. Hampe, I. Kojima, R. Schwarz, and H.C. Schaller. 2001. The neuropeptide head activator induces activation and translocation of the growth-factor-regulated Ca^{2+}-permeable channel GRC. *J. Cell Sci.* 114:3599–3606.

Brown, S.C., and J.A. Lucy. 1997. Functions of dystrophin. *In* Dystrophin. Gene, Protein and Cell Biology. S.C. Brown and J.A. Lucy, editors. Cambridge University Press, Cambridge. 163–200.

Caterina, M.J., T.A. Rosen, M. Tominaga, A.J. Brake, and D. Julius. 1997. The capsaicin receptor: a heat-activated ion channel in the pain pathway. *Nature.* 389:816–824.

Caterina, M.J., T.A. Rosen, M. Tominaga, A.J. Brake, and D. Julius. 1999. A capsaicin-receptor homologue with a high threshold for noxious heat. *Nature.* 398:436–441.

Cullen, M.J., and J.J. Fulthorpe. 1975. Stages in fiber breakdown in Duchenne muscular dystrophy. An electron-microscopic study. *J. Neurol. Sci.* 24:179–200.

Cullen, M.J., and E. Jaros. 1988. Ultrastructure of the skeletal muscle in the X chromosome-linked dystrophic (mdx) mouse. Comparison with Duchenne muscular dystrophy. *Acta Neuropathol. (Berl).* 77:69–81.

Delaughter, M.C., G.E. Taffet, M.L. Fiorotto, M.L. Entman, and R.J. Schwartz. 1999. Local insulin-like growth factor I expression induces physiologic, then pathologic, cardiac hypertrophy in transgenic mice. *FASEB J.* 13:1923–1929.

Duerr, R.L., S. Huang, H.R. Miraliakbar, R. Clark, K.R. Chien, and J. Ross, Jr. 1995. Insulin-like growth factor-1 enhances ventricular hypertrophy and function during the onset of experimental cardiac failure. *J. Clin. Invest.* 95:619–627.

Fong, P.Y., P.R. Turner, W.F. Denetclaw, and R.A. Steinhardt. 1990. Increased activity of calcium leak channels in myotubes of Duchenne human and mdx mouse origin. *Science.* 250:673–676.

Franco-Obregon, A., Jr., and J.B. Lansman. 1994. Mechanosensitive ion channels in skeletal muscle from normal and dystrophic mice. *J. Physiol.* 481:299–309.

Grynkiewicz, G., M. Poenie, and R.Y. Tsien. 1985. A new generation of calcium indicators with greatly improved fluorescence properties. *J. Biol. Chem.* 260:3440–3450.

Iwata, Y., H. Nakamura, Y. Mizuno, M. Yoshida, E. Ozawa, and M. Shigekawa. 1993. Defective association of dystrophin with sarcolemmal glycoproteins in the cardiomyopathic hamster heart. *FEBS Lett.* 329:227–231.

Iwata, Y., Y. Pan, H. Hanada, T. Yoshida, and M. Shigekawa. 1996. Dystrophin–glycoprotein complex purified from hamster cardiac muscle. Comparison of the complexes from cardiac and skeletal muscles of hamster and rabbit. *J. Mol. Cell. Cardiol.* 28:2501–2509.

Kanzaki, M., Y.Q. Zhang, H. Mashima, H. Shibata, and I. Kojima. 1999. Translocation of a calcium-permeable cation channel induced by insulin-like growth factor-1. *Nat. Cell Biol.* 1:165–170.

MacLennan, P.A., A. McArdle, and R.H.T. Edwards. 1991. Effects of calcium on protein turnover of incubated muscles from mdx mice. *Am. J. Physiol.* 260:E594–E598.

Mallouk, N., V. Jacquemond, and B. Allard. 2000. Elevated subsarcolemmal Ca^{2+} in mdx mouse skeletal muscle fibers detected with Ca^{2+}-activated K^+ channels. *Proc. Natl. Acad. Sci. USA.* 97:4950–4955.

Menke, A., and H. Jockusch. 1991. Decreased osmotic stability of dystrophin-less muscle cells from the mdx mouse. *Nature.* 349:69–71.

Mokri, B., and A.G. Engel. 1975. Duchenne dystrophy: electronic microscopic findings pointing to a basic or early abnormality in the plasma membrane of muscle fiber. *Neurology.* 25:1111–1120.

Montell, C., and L. Birnbaumer. 2002. The TRP channels, a remarkably functional family. *Cell.* 108:595–598.

Nakamura, T.Y., Y. Iwata, M. Sampaolesi, H. Hanada, N. Saito, M. Artman, W.A. Coetzee, and M. Shigekawa. 2001. Stretch-activated cation channels in skeletal muscle myotubes from sarcoglycan-deficient hamsters. *Am. J. Physiol. Cell Physiol.* 281:C690–C699.

Naruse, K., T. Yamada, and M. Sokabe. 1998. Involvement of SA channels in orienting response of cultured endothelial cells to cyclic stretch. *Am. J. Physiol.* 274:H1532–H1538.

Nigro, V., Y. Okazaki, A. Belsito, G. Piluso, Y. Matsuda, L. Politano, G. Nigro, C. Ventura, C. Abbondanza, A.M. Molinari, et al. 1997. Identification of the Syrian hamster cardiomyopathy gene. *Hum. Mol. Genet.* 6:601–607.

Ozawa, E., S. Noguchi, Y. Mizuno, Y. Hagiwara, and M. Yoshida. 1998. From dystrophinopathy to sarcoglycanopathy: evolution of a concept of muscular dystrophy. *Muscle Nerve.* 21:421–438.

Petrof, B.J., J.B. Shrager, H.H. Stedman, A.M. Kelly, and H.L. Sweeney. 1993. Dystrophin protects the sarcolemma from stresses developed during muscle contraction. *Proc. Natl. Acad. Sci. USA.* 90:3710–3714.

Rando, T.A., and H.M. Blau. 1994. Primary mouse myoblast purification, characterization, and transplantation for cell-mediated gene therapy. *J. Cell Biol.* 125:1275–1287.

Reimer, K.A., and R.B. Jenning. 1986. Myocardial ischemia, hypoxia, and infarction. *In* The Heart and Cardiovascular System. H.A. Fozzard, E.H. Habor, R. B. Jennings, A.M. Katz, and H.E. Morgan, editors. Raven Press, New York. 1133–1202.

Robert, V., M.L. Massimino, V. Tosello, R. Marsault, M. Cantini, V. Sorrentino, and T. Pozzan. 2001. Alteration in calcium handling at the subcellular level in mdx myotubes. *J. Biol. Chem.* 276:4647–4651.

Saito, S., Y. Hiroi, Y. Zou, R. Aikawa, H. Toko, F. Shibasaki, Y. Yazaki, R. Nagai, and I. Komuro. 2000. β-Adrenergic pathway induces apoptosis through calcineurin activation in cardiac myocytes. *J. Biol. Chem.* 275:34528–34533.

Sampaolesi, M., Y. Yoshida, Y. Iwata, H. Hanada, and M. Shigekawa. 2001. Stretch-induced cell damage in sarcoglycan-deficient myotubes. *Pflugers Arch.* 442:161–170.

Shirinsky, V.P., A.S. Antonov, K.G. Birukov, A.V. Sobolevsky, Y.A. Romanov, N.V. Kabaeva, G.N. Antonova, and V.N. Smirnov. 1989. Mechano-chemi-

cal control of human endothelium orientation and size. *J. Cell Biol.* 109: 331–339.

Spencer, M.J., D.E. Croall, and J.G. Tidball. 1995. Calpains are activated in necrotic fibers from mdx dystrophic mice. *J. Biol. Chem.* 270:10909–10914.

Stewart, C., and P. Rotwein. 1996. Growth, differentiation, and survival: multiple physiological functions for insulin-like growth factors. *Physiol. Rev.* 76: 1005–1026.

Straub, V., and K.P. Campbell. 1997. Muscular dystrophies and the dystrophin-glycoprotein complex. *Curr. Opin. Neurol.* 10:168–175.

Suzuki, M., J. Sato, K. Kutsuwada, G. Ooki, and M. Imai. 1999. Cloning of a stretch-inhibitable nonselective cation channel. *J. Biol. Chem.* 274:6330–6335.

Torres, L.F., and L.W. Duchen. 1987. The mutant mdx: inherited myopathy in the mouse. Morphological studies of nerves, muscles and end-plates. *Brain.* 110:269–299.

Towbin, J.A., and N.E. Bawles. 2002. The failing heart. *Nature.* 415:227–233.

Turner, P.R., T. Westwood, C.M. Regen, and R.A. Steinhardt. 1988. Increased protein degradation results from elevated free calcium levels found in muscle from *mdx* mice. *Nature.* 335:735–738.

Tutdibi, O., H. Brinkmeier, R. Rudel, and K.J. Föhr. 1999. Increased calcium entry into dystrophin-deficient muscle fibers of MDX and ADR-MDX mice is reduced by ion channel blockers. *J. Physiol.* 515:859–868.

Vandebrouck, C., G. Dupont, C. Cognard, and G. Raymond. 2001. Cationic channels in normal and dystrophic myotubes. *Neuromuscul. Disord.* 11:72–79.

Vandebrouck, C., D. Martin, M. Colson-Van Schoor, H. Debaix, and P. Gailly. 2002. Involvement of TRPC in the abnormal calcium influx observed in dystrophic (mdx) mouse skeletal muscle fibers. *J. Cell Biol.* 158:1089–1096.

Wakabayashi, S., T. Pang, X. Su, and M. Shigekewa. 2000. A novel topology model of the human Na^+/H^+ exchanger isoform 1. *J. Biol. Chem.* 275: 7942–7949.

Yoshida, T., Y. Pan, H. Hanada, Y. Iwata, and M. Shigekawa. 1998. Bidirectional signaling between sarcoglycans and the integrin adhesion system in cultured L6 myocytes. *J. Biol. Chem.* 273:1583–1590.